Chinese Chemical Letters 35 (2024) 108384

Contents lists available at ScienceDirect

Chinese Chemical Letters

journal homepage: www.elsevier.com/locate/cclet

Applying dynamic light scattering to investigate the self-assembly process of DNA nanostructures

Wei Yuan[a,b], Gui-Zhi Dong[a,b], Hui Ning[c], Xiang-Xiang Guan[d], Jia-Feng Cheng[e], Zi-Wei Shi[a,b], Xiu-Ji Du[a,b], Si-Wen Meng[a,b], Dong-Sheng Liu[d], Yuan-Chen Dong[a,b,*]

[a] CAS Key Laboratory of Colloid, Interface and Chemical Thermodynamics, Institute of Chemistry, Chinese Academy of Sciences, Beijing 100190, China
[b] University of Chinese Academy of Sciences, Beijing 100049, China
[c] Dandong Bettersize Instruments Ltd., Dandong 118000, China
[d] Key Laboratory of Organic Optoelectronics & Molecular Engineering of the Ministry of Education, Department of Chemistry, Tsinghua University, Beijing 100084, China
[e] Department of Chemistry, Renmin University of China, Beijing 100872, China

ARTICLE INFO

Article history:
Received 28 February 2023
Revised 23 March 2023
Accepted 26 March 2023
Available online 28 March 2023

Keywords:
Dynamic light scattering
Self-assembly process
DNA nanostructures
Temperature transition ranges
Rapid preparation

ABSTRACT

Understanding the dynamic assembly process of DNA nanostructures is important for developing novel strategy to design and construct functional devices. In this work, temperature-controlled dynamic light scattering (DLS) strategy has been applied to study the global assembly process of DNA origami and DNA bricks. Through the temperature dependent size and intensity profiles, the self-assembly process of various DNA nanostructures with different morphologies have been well-studied and the temperature transition ranges could be observed. Taking advantage of the DLS information, rapid preparation of the DNA origami and the brick assembly has been realized through a constant temperature annealing. Our results demonstrate that the DLS-based strategy provides a convenient and robust tool to study the dynamic process of forming hieratical DNA structures, which will benefit understanding the mechanism of self-assembly of DNA nanostructures.

In last few decades, DNA nanotechnology has expanded a new area to construct defined two-dimensional (2D) and three-dimensional (3D) nanostructures with predesigned shapes and sizes [1–10]. Taking advantage of the specificity and addressability of DNA assembly, diverse functional nanodevices, including biosensors [11–14], nanorobots [15–18], and reconfigurable nanostructures [19–21], have been also realized. While the design and construction of the DNA assembly has been widely investigated, understanding the dynamic of DNA assembly process is also of great importance, which will benefit understanding the synergistic mechanism of the precise assembly of the macro-biomolecules. However, investigation in the dynamic process is still challenged by lack of efficient tools.

Recently, several methods have been developed to study the thermodynamics and kinetics of DNA self-assembly [22–36]. Ultraviolet–visible spectroscopy (UV–vis) method [26,27] relied on the different absorbance between the single strands and duplex at 260 nm, which was useful for study the formation of the DNA helix but suffered from a poor accuracy in complex DNA system. Fluorescent technology [28–31] has also been applied to reveal the thermal folding and unfolding of 3D DNA origami nanostructures. While more detailed information could be achieved, the position of the fluorescent molecules could affect the detected results and the expensive chemical modifications also limited the potential applications. Atomic force microscope (AFM) [32–35] could visualize the formation of a DNA origami structure under relatively coarse temperature control, however, the manipulation at a solid-liquid interface of AFM may not reflect the formation process in solution. Moreover, while AFM exhibits advantage of the study in 2D structures, the more complexed 3D structures have not been investigated. Recently, static light scattering (SLS) [36] has been employed to investigate the folding and unfolding of DNA origamis, which has shown preponderance in detection and characterization of molecular mass. However, it is also necessary to obtain other important structure information for more precise analysis of the DNA assembly process.

Dynamic light scattering (DLS) is a robust technology to characterize the particle size and size distribution of samples on the nanoscale. When the nanoparticles are dispersed in aqueous media, the random Brownian motion results in time-progressive

* Corresponding author.
E-mail address: dongyc@iccas.ac.cn (Y.-C. Dong).

https://doi.org/10.1016/j.cclet.2023.108384
1001-8417/

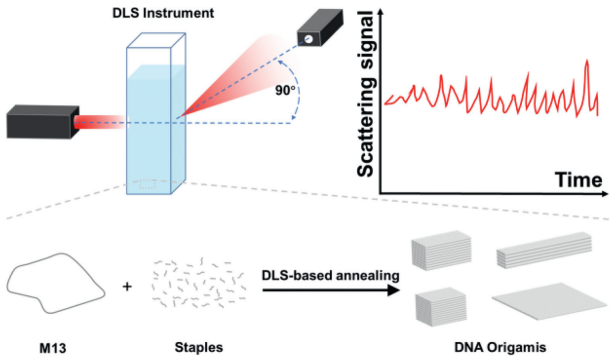

Scheme 1. Self-assembly process of DNA nanostructures was monitored by DLS strategy during the annealing process.

fluctuations of the scattered light under laser beam illuminating. The time-dependent scattering intensity fluctuation is converted to correlation function by correlator, the average size and size distribution of the nanoparticles can be calculated by cumulants and multiple exponential algorithms, respectively. Based on the DLS method, the time-dependent size change of the monitored nanoparticle could be achieved [37–39]. Recently, the temperature-dependent dynamic self-assembly behavior of the nonlinear block polymers has been well-studied, which has shown a promise potential for investigating the dynamic assembly of various nanoparticles [40–42]. Here in this study, we utilized the DLS strategy to study the self-assembly of DNA nanostructures by investigating the temperature dependent of both size and light intensity. The temperature transitions of particle size and scattering intensity in different structures have been observed, which has been demonstrated to be important indicators in the formation of DNA origami. Furthermore, DNA bricks-based nanostructures has also been investigated through DLS and indicated a different nucleation mechanism, which will help us understand the mechanism of self-assembly of complex DNA nanostructures.

To investigate the DNA assembly process through DLS, as illustrated in Scheme 1, we firstly monitored the formation of a 3D DNA origami as a typical example in real-time temperature ramp mode. DNA origami conceptually folds a long single strand as scaffold into pre-designed structures by hundreds of short staples strands DNA, which provides a powerful tool for constructing customized nanostructures. Here we chose a well-established 3D DNA cubic origami (termed as O1) as an example with the size of 20 nm × 20 nm × 40 nm (detailed design and sequence information could be found in Supporting information). In our experiments, a 7249-nt single stranded M13 (20 nmol/L) was selected as the scaffold strand and incubated with 200 nmol/L short staple strands. Then the mixed solution was applied to DLS under an annealing process from 85 °C to 25 °C with a cooling rate of 1 °C per step and the sample maintained equilibrium for 10 min at each step. During the annealing process, the dimension (diameter, number averaged) information was detected and recorded.

As shown in Fig. 1a, from 85 °C to 50 °C, the diameter almost kept in a range of 3.5 nm during cooling process. With further cooling process, a sharp size change to 30 nm was observed around 49 °C. To exclude size effect of the long scaffold strand and staples, control experiments were evaluated, and as shown in Fig. S1 (Supporting information), no obvious size change was observed both in only M13 group or only staples group during the annealing process. These results demonstrated that sharp size change of the experimental group was attributed to the origami formation.

To further illustrate the dynamic process and avoid the unexpected environmental effect, the intensity correlation function and average scattering light intensity were also recorded and analyzed during the annealing process. As illustrated in Fig. 1b, compared with the sharp transition in the size distribution, the time-dependent intensity correlation function was observed with placid change, which indicated relatively gradual transfomation of the particles in the system. The zoomed and detailed image of the correlation function has also been provided in the Fig. S2 (Supporting information) to reveal the formation process of the O1. The smooth changes in the profiles have been found between 48 °C and 50 °C, which suggested that the process of forming the DNA nanostructures in this temperature range underwent tardily. Consistent with the results of intensity correlation function, a smooth curve was detected and the intensity increased upon the decreased temperature from 50 °C to 40 °C (Fig. 1c), which could be also explained by formation of the origami. As control, no obvious intensity change was detected in only M13 solution or only staples group during the annealing (Fig. S3 in Supporting information). Taken together, the O1-based results have demonstrated the formation of the DNA origami induced the change of the diameter and scattering intensity.

It has been recognized that while we used the number averaged size in the size plot which reflects the average size of the largest number population of particles, the contribution from the minor amount of large aggregates would be neglected. Therefore, the scattering intensity curve could provide more comprehensive contribution from particle density which affects dn/dc, the scattering ability, and size distribution of total particles in detected systems. In the origami system, the content of target DNA structures could be considered as a constant due to the fixed concentration of scaffold (M13). The sharp transition in the temperature dependent diameter curve might be attributed to the transition states of the assembly, but it could not reveal the completed formation of the origami. On the other hand, the smooth transition from 50 °C to 40 °C under the intensity curve could be explained that the intact DNA origami was gradually formed in such temperature range and the constant density after 40 °C indicated the successful formation of O1. These results demonstrated that DLS could facilitate the investigation of the dynamic assembly process and revealing of the important role of the temperature effect.

Moreover, the disassembled process of the formed O1 was also explored for proving the robustness of DLS strategy. Both the temperature dependent diameter and scattering intensity curves showed that the formed O1 was stable below 50 °C. As illustrated in Fig. S4 (Supporting information), the obvious hysteresis phenomenon of disassembly of O1 could be observed when heated above 50 °C and a higher temperature transition range from 50 °C to 60 °C has been recorded, which could be attributed to collaborative effects that the staples remained to maintain the folded structure. These results have confirmed that the disassembly process of O1 could be also well-monitored by robust DLS method.

To confirm the successful formation of the origami on the DLS instruments, the sample was characterized by agarose gel electrophoresis and transmission electron microscope (TEM). A traditional annealing method on PCR instrument (detailed information in Supporting information) was also employed as a positive control. The sample prepared on the DLS instrument showed the identical migration rate with the well-established PCR group in the agarose gel, which proved the intact structures were formed (Fig. S5a in Supporting information). Furthermore, as shown in Fig. 1d, ordered DNA origami structures could be also observed under TEM, which was comparable to TEM result of PCR group (Fig. S5b in Supporting information) and well-consistent with the design. These results demonstrated that the well-defined DNA origami has been prepared, which further supported the DLS-based data.

To verify the importance of the temperature transition range as indicated in the temperature dependent intensity curve, we conducted a series of assembly experiment under constant tem-

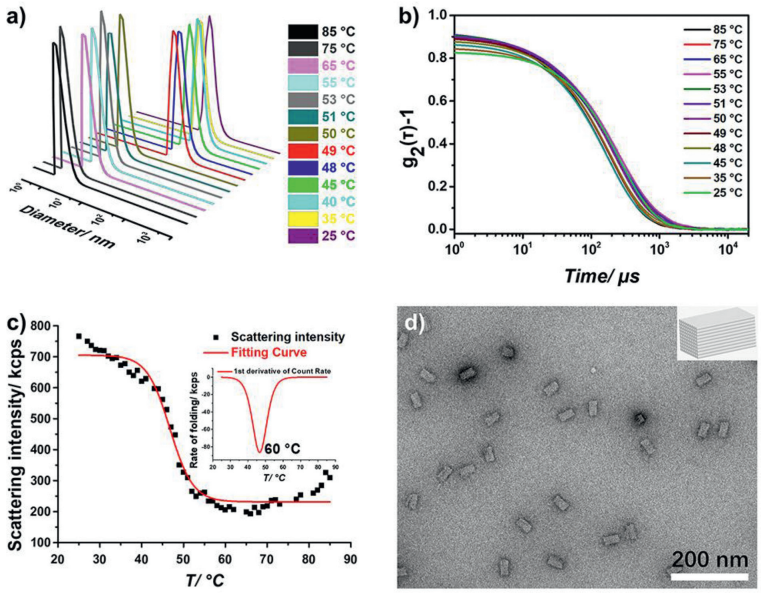

Fig. 1. Self-assembly process of O1 monitored through DLS. (a) Size distribution of O1 at different temperatures during the annealing process. (b) The curves of time dependent intensity correlation function at different temperatures. (c) Temperature dependent scattering intensity curve during the annealing procedure. (d) TEM image of O1 after annealing process on the DLS instruments. The insert figure showed the schematic morphology of the O1. The scale bar is 200 nm.

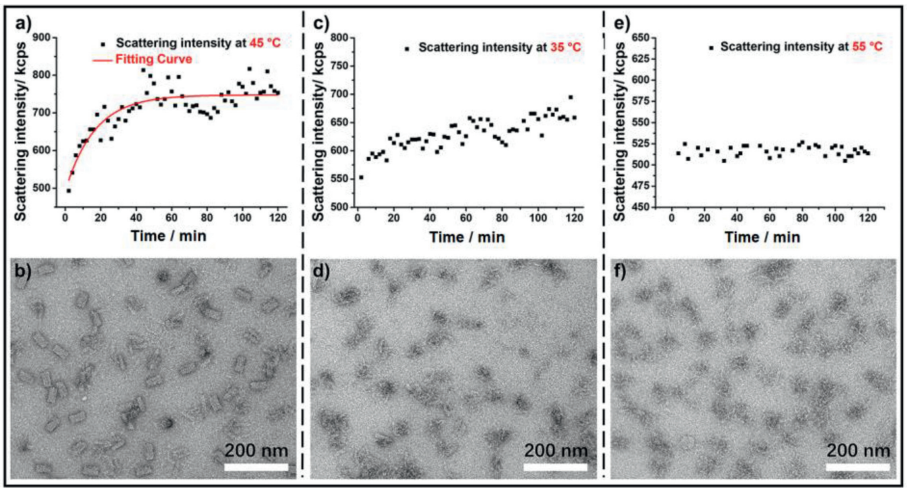

Fig. 2. Self-assembly of O1 at constant temperatures. (a) Time dependent scattering intensity curve during the constant incubation of O1 at 45 °C and (b) its TEM image. (c) Time dependent scattering intensity curve during the constant incubation at 35 °C and (d) its TEM image. (e) Time dependent scattering intensity curve during the constant incubation at 55 °C and (f) its TEM image. The scale bar is 200 nm.

peratures and the scattering intensity was constantly monitored for 2 h. As shown in Fig. 2a, the rapid increase of scattering intensity was observed in the first 40 min at 45 °C, which indicated the origami was folded rapidly under such temperature (Fig. S6 in Supporting information). After DLS measurement, intact and shape-defined origami structure could be observed under the TEM as illustrated in Fig. 2b, which was consistent with the DLS data. It should be mentioned that, as illustrated in Fig. S7 (Supporting information), time-dependent formation experiment characterized at 45 °C was also investigated by TEM, which further proved that the intact origamis were well-formed after 45 min incubation. In addition to 45 °C, the incubation at other temperatures in the detected temperature transition range (50 °C to 40 °C) was also investigated, and similar results have been observed (Fig. S8 in Supporting information). On the other hand, under the incubation below or above the temperature transition range (35 °C and 55 °C), there was no obvious change in scattering intensity or diameter during the assembly process (Figs. 2c and e). The TEM experiments also demonstrated that no regular structures could be observed in these conditions (Figs. 2d and f). These results demonstrated that DLS could provide a convenient strategy to the investigate the dynamic folding process and the proper temperature transition range for formation of the origami was also revealed through such tool.

To further demonstrate the versatility of the DLS strategy, a cubic origami (O2, 25 nm × 25 nm × 30 nm) and another 3D rod-like (O3, 10 nm × 10 nm × 60 nm) were also investigated (Fig. 3). The experiments were carried out under identical procedure with same concentration as O1. As shown in Fig. S9 (Supporting information), the O2 showed an obvious change in diameter when the temperature cooled to 48 °C, and gradual increase in scattering intensity curve was recorded from 55 °C to 40 °C (Fig. 3a). Similar results of the origami formation were observed in O3 detected system (Fig. 3c, Fig. S10 in Supporting information). After detection, the samples were also studied by TEM and the intact structures as predesigned were observed in both systems (Figs. 3b and d). Subsequently, the constant temperature assembly experiments

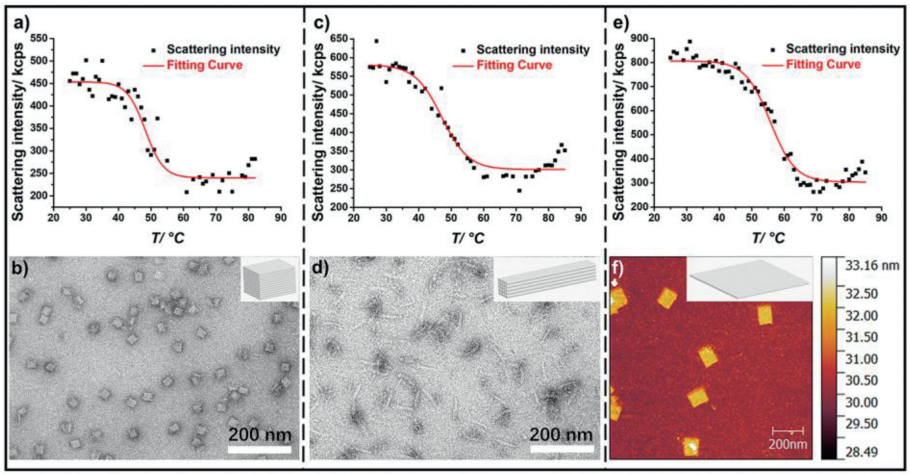

Fig. 3. Versatility of DLS strategy to reveal the formation of different origamis. (a, c, e) Temperature dependent scattering intensity curves of O2, O3 and O4, respectively, during the annealing process. (b, d) TEM images of assembly result of O2, O3 after the annealing procedure, respectively. The insert figures showed the schematic morphologies of the O2 and O3, respectively. The scale bar is 200 nm. (f) AFM image of O4-based assembly result after DLS-based annealing procedure. The insert figure showed the schematic morphology of the O4.

were also conducted. Consistent with O1, well-assembled O2 and O3 could be observed in TEM images (Figs. S11 and S12 in Supporting information) after incubation at the selected temperature (48 °C for O2, 43 °C for O3) or PCR based annealing. These results further supported that DLS could provide a robust tool to monitor dynamic assembly of origamis with different morphologies.

In addition to 3D origami structures, we have also applied DLS to investigate the two-dimensional DNA origami structure. Compared to the rigid 3D structure, a more flexible planar rectangular origami (O4) with 60 nm × 70 nm (Fig. 3) was designed and the dynamic assembly process was monitored. As shown in Fig. 3e, O4 showed an increase of temperature dependent scattering intensity with a temperature transition range from 65 °C to 45 °C, and similar change tendency was observed in diameter curve (Fig. S13 in Supporting information). After test, the sample was also studied by TEM (Fig. S14a in Supporting information), which agreed well with DLS experiment. It should be noted that under TEM, the curled structures of O4 could be attributed to the flexible property of the 2D origami. Therefore, AFM was also employed and the shape-defined and uniform nanosheets could be clearly observed (Fig. 3f). Furthermore, the constant incubation experiments under 55 °C were also conducted and the intact O4 has also been characterized by TEM (Fig. S14b in Supporting information). The results were well-consistent with the DLS-based TEM result, which further suggested that the dynamic self-assembly of 2D origami could be also well-monitored by versatile DLS strategy.

Recently, a DNA brick method has also been proposed to fabricate the defined DNA structures assembly *via* only short strands, which was also investigated in our study through DLS. A targeted 3D cubic structure called D1 (Fig. 4a) with a diameter of 15 nm × 15 nm × 35 nm was selected, and 200 nmol/L bricks were annealing from 80 °C to 25 °C with a constant cooling rate of 1 °C per 20 min. As showed in Fig. 4b, significant change of diameter of D1-based system could be observed at a temperature about 36 °C, which indicated the targeted structure begun to form. The similar tendency was observed in temperature dependent intensity curve (Fig. 4c), a temperature transition range from 37 °C to 33 °C could been seen. To confirm the formation under DLS annealing, TEM characterization was also conducted. As shown in Fig. 4d, well-defined targeted structure with predesigned size and shape could be clearly seen.

Furthermore, the time dependent incubation of the bricks under 35 °C was also studied by DLS and characterized by agarose gel electrophoresis. As shown in Fig. S15 (Supporting information), little intensity change was recorded at the first 2 h. The scattering intensity dramatically increased from 3 h to 6 h, and then stabilized at constant value. Consistent with the DLS result, a weak band of targeted DNA nanostructure could be found (Fig. S16 in Supporting information) after 2 h incubation, and the yield was obviously increased after 6 h incubation. With further incubation to 8 h, the yield of D1 comparable to that of PCR group could be achieved. To prove indeed formation of the intact D1, the samples were further studied by TEM. As shown in Fig. S17 (Supporting information), the small proportion of well-formed D1 could be seen after 2 h, but increased yield could be observed with further incubation to 6 h, and comparable yield to PCR could be achieved with further incubation to 8 h. Compared to the assembly mediated by long scaffold, the relative low formation speed of D1 indicated that the assembly of the small bricks underwent a different pathway, which was also consistent with the previous assumption that sparse and slow nucleation was involved, then followed by fast growth to the intact assembly [43]. These results suggested that DLS could be also utilized to monitor the relatively slow assembly process of the DNA bricks, which has been proven to be a versatile method to investigate the assembly process of different DNA nanostructures.

In conclusion, we have applied DLS to investigate the dynamic assembly process of DNA nanostructures including DNA origami and DNA bricks. Both the temperature dependent size and scattering intensity curves have been analyzed, and the increased average diameters and intensity have been detected upon the annealing process of the DNA origami. While the size curve of DLS directly reflects the size change of the particles with temperature, the scattering intensity curve provides the combined information of particle density, size distribution and scattering ability. Therefore, the transition range in the intensity mode may indicate the gradual formation of the intact DNA origami in such temperature region. Benefiting from the information of DLS, a rapid and easy assembly strategy of DNA origami in half an hour has been optimized under a constant temperature. Furthermore, the assembly process of the DNA bricks-based nanostructures has also been investigated through DLS. While similar transition range has also been observed, the constant annealing assembly results indicated a more complex pathway, where a potential slow and subtle nucleation process might be involved. Our results have demonstrated that DLS could facilitate the investigation of the dynamic assembly process of the DNA nanostructures. The DLS technology has

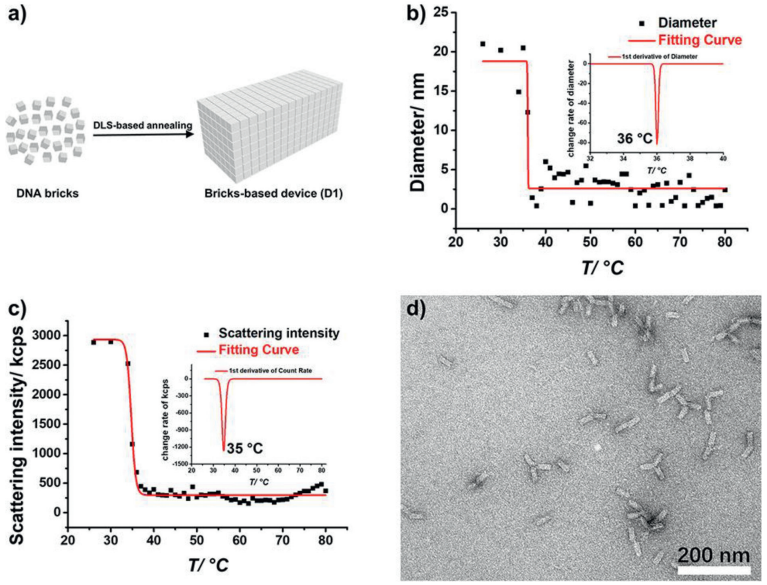

Fig. 4. DLS monitored self-assembly process of DNA bricks. (a) The schematic planar rectangular structure of D1. (b) Temperature dependent diameter curve of D1. (c) Temperature dependent scattering intensity curve of D1. (d) TEM image of D1-based assembly result after DLS-based annealing procedure. The scale bar is 200 nm.

been demonstrated to provide label-free, robust and convenient tool to study the dynamic process of the complex DNA assembly. Furthermore, the manipulation of the DLS is unsophisticated and the structure information can be obtained simultaneously upon the dimension transition, which will reveal more accurate and useful clues for analyzing the dynamic assembly. While more efforts should be paid in understanding the DLS data for complex system, it can still be anticipated that, combined with fluorescence resonance energy transfer (FRET) and cryogenic electron microscopy (cryo-EM), more effective information could be achieved, which will benefit understanding the mechanism of self-assembly of DNA nano-structures.

Declaration of competing interest

The authors declare that they have no known competing financial interests or personal relationships that could have appeared to influence the work reported in this paper.

Acknowledgment

This work was supported by the National Natural Science Foundation of China (No. 21971248).

Supplementary materials

Supplementary material associated with this article can be found, in the online version, at doi:10.1016/j.cclet.2023.108384.

References

[1] E. Winfree, F. Liu, L.A. Wenzler, et al., Nature 394 (1998) 539–544.
[2] N.C. Seeman, Nature 421 (2003) 427–431.
[3] P.W. Rothemund, Nature 440 (2006) 297–302.
[4] S.M. Douglas, H. Dietz, T. Liedl, et al., Nature 459 (2009) 414–418.
[5] D. Han, S. Pal, J. Nangreave, et al., Science 332 (2011) 342–346.
[6] Y. Ke, L.L. Ong, W.M. Shih, et al., Science 338 (2012) 1177–1183.
[7] S. Dey, C. Fan, K. Gothelf, et al., Nat. Rev. Methods Primers 1 (2021) 1–24.
[8] S.M. Douglas, A.H. Marblestone, S. Teerapittayanon, et al., Nucl. Acids Res. 37 (2009) 5001–5006.
[9] H. Jun, X. Wang, M.F. Parsons, et al., Nucl. Acids Res. 49 (2021) 10265–10274.
[10] J. Piao, W. Yuan, Y. Dong, Macromol. Biosci. 21 (2021) e2000440.
[11] M. Marini, L. Piantanida, R. Musetti, et al., Nano Lett. 11 (2011) 5449–5454.
[12] A. Kuzuya, Y. Sakai, T. Yamazaki, et al., Nat. Commun. 2 (2011) 449.
[13] H.K. Subramanian, B. Chakraborty, R. Sha, et al., Nano Lett. 11 (2011) 910–913.
[14] H. Yu, T. Man, W. Ji, et al., Chin. Chem. Lett. 30 (2019) 175–178.
[15] A.J. Thubagere, W. Li, R.F. Johnson, et al., Science 357 (2017) eaan6558.
[16] S.M. Douglas, I. Bachelet, G.M. Church, Science 335 (2012) 831–834.
[17] K. Lund, A.J. Manzo, N. Dabby, et al., Nature 465 (2010) 206–210.
[18] L. Li, K. Dong, X. Wang, et al., Chin. Chem. Lett. 33 (2022) 2052–2056.
[19] Y. Liu, J. Cheng, S. Fan, et al., Angew Chem. Int. Ed. 59 (2020) 23277–23282.
[20] F. Zhang, J. Nangreave, Y. Liu, et al., Nano Lett. 12 (2012) 3290–3295.
[21] D. Han, S. Pal, Y. Liu, et al., Nat. Nanotechnol. 5 (2010) 712–717.
[22] W. Bae, K. Kim, D. Min, et al., Nat. Commun. 5 (2014) 5654.
[23] C. Liang, J. Chen, M. Li, et al., Chem. Commun. 58 (2022) 8352–8355.
[24] V.R. Harkness, N. Avakyan, H.F. Sleiman, et al., Nat. Commun. 9 (2018) 3152.
[25] S. Fischer, C. Hartl, K. Frank, et al., Nano Lett. 16 (2016) 4282–4287.
[26] T.L. Sobey, S. Renner, F.C. Simmel, J. Phys. Condens. Matter 21 (2009) 034112.
[27] L.A. Marky, K.J. Breslauer, Biopolymers 26 (1987) 1601–1620.
[28] X. Wei, J. Nangreave, S. Jiang, et al., J. Am. Chem. Soc. 135 (2013) 6165–6176.
[29] J.-P.J. Sobczak, T.G. Martin, T. Gerling, et al., Science 338 (2012) 1458–1461.
[30] P. Huang, J. Wang, L. Jiao, et al., Biosens. Bioelectron. 131 (2019) 224–231.
[31] J.M. Majikes, P.N. Patrone, D. Schiffels, et al., Nucl. Acids Res. 48 (2020) 5268–5280.
[32] J. Song, J.M. Arbona, Z. Zhang, et al., J. Am. Chem. Soc. 134 (2012) 9844–9847.
[33] J. Song, Z. Zhang, S. Zhang, et al., Small 9 (2013) 2954–2959.
[34] J.L. Wah, C. David, S. Rudiuk, et al., ACS Nano 10 (2016) 1978–1987.
[35] J. Wang, Y. Wei, P. Zhang, et al., Nano Lett. 22 (2022) 7173–7179.
[36] H. Ijäs, T. Liedl, V. Linko, et al., Biophys. J. 121 (2022) 4800–4809.
[37] X. Miao, S. Zou, H. Zhang, et al., Sens. Actuators B: Chem. 191 (2014) 396–400.
[38] C. Wang, J. Piao, Y. Li, et al., Angew. Chem. Int. Ed. 59 (2020) 15176–15180.
[39] R. Schubert, A. Meyer, D. Baitan, et al., Cryst. Growth Des. 17 (2017) 954–958.
[40] H.W. Chen, J.F. Li, Y.W. Ding, et al., Macromolecules 38 (2005) 4403–4408.
[41] S. Sun, P. Wu, W. Zhang, et al., Soft Matter 9 (2013) 1807–1816.
[42] K.K. Sharker, S. Takeshima, Y. Toyama, et al., Polymer 203 (2020) 122735.
[43] B. Wei, M. Dai, P. Yin, Nature 485 (2012) 623–626.